This report is a living document and will be updated as required, the current version is dated 7 April 2018.

Benchmark Problem Definition and Cross-Validation for Characteristic Mode Solvers

Yikai Chen[1], Kurt Schab[2], Miloslav Čapek[3], Michal Mašek[3], Buon Kiong Lau[4], Hanieh Aliakbari[4], Yigit Haykir[5], Qi Wu[6], W.J. Strydom[7], Nikolai Peitzmeier[8], Milos Jovicic[9], Simone Genovesi[10], Francesco Alessio Dicandia[10]

[1] University of Electronic Science and Technology of China, Chengdu, China, ykchen@uestc.edu.cn

[2] North Carolina State University, Raleigh, USA, krschab@ncsu.edu

[3] Czech Technical University, Prague, Czech Republic, miloslav.capek@fel.cvut.cz

[4] Lund University, Lund, Sweden, buon_kiong.lau@eit.lth.se

[5] Middle East Technical University, Ankara, Turkey, yigit.haykir@metu.edu.tr

[6] Beihang University, Beijing, China, qwu@buaa.edu.cn

[7] Altair Development S.A. (Pty) Ltd, Stellenbosch, South Africa, wstrydom@altair.co.za

[8] Leibniz Universität Hannover, Hannover, Germany, peitzmeier@hft.uni-hannover.de

[9] WIPL-D d.o.o., Belgrade, Serbia, milos.jovicic@wipl-d.com

[10] Università di Pisa, Pisa, Italy, simone.genovesi@iet.unipi.it; alessio.dicandia@for.unipi.it

***Abstract*— In October 2016, the Special Interest Group on Theory of Characteristic Modes (TCM) initiated a coordinated effort to perform benchmarking work for characteristic mode (CM) analysis. The primary purpose is to help improve the reliability and capability of existing CM solvers and to provide the means for validating future tools. Significant progress has already been made in this joint activity. In particular, this paper describes several benchmark problems that were defined and analyzes some results from the cross-validations of different CM solvers using these problems. The results show that despite differences in the implementation details, good agreement is observed in the calculated eigenvalues and eigencurrents across the solvers. Finally, it is concluded that future work should focus on understanding the impact of common parameters and output settings to further reduce variability in the results.**

***Index Terms*— Characteristic modes, benchmark problems, electromagnetic modeling**

I. INTRODUCTION

The theory of characteristic modes (TCM) [1], [2] is becoming increasingly popular for analyzing electro-magnetic radiation and scattering problems in the early stages of research and development. This is because it provides scientists and engineers a helpful tool to capture the physical mechanisms underlying these electromagnetic phenomena [3]-[8]. Moreover, in recent years, significant progress has been made in the development of characteristic mode (CM) solvers for internal research and commercial developments [6]. These tools have facilitated the extensive use of CM analysis (CMA) to assist in the design and implementation of many different antenna structures, e.g., [3]-[6].

Despite significant advances in CM research, there is little benchmarking information available for CMA. Electromagnetic numerical modeling code and technique standardization is an important topic to the electromagnetics community [9], as evidenced through numerous papers on a wide range of numerical modeling techniques (see [10] and references therein). CM benchmarking development is also critical for further advancing this field as it will provide a clear picture of the strengths and weaknesses of existing algorithm and spur new algorithm development. Extensive code validations, especially cross validations, are required to place confidence in the results that are produced by both in-house and commercially available CMA software tools.

As a step forward, the performance of several state-of-the-art commercial and in-house CMA tools were investigated in [11]. CM solutions for a perfectly electric conductor (PEC), i.e., a sphere, were computed and compared to the analytical solution. The results show that singularity treatment, quadrature rules, mesh size, and electrical size of the problem of interest may greatly influence the accuracy of the solved modes. To support CM benchmarking development, the Special Interest Group (SIG) on TCM [12] initiated benchmarking activities that aim to provide a suite of problems that test, not only accuracy, but also robustness of existing CM solvers in handling arbitrarily shaped problems with a variety of input parameters.

In this paper, three benchmark problems are considered. To focus on the most common and accessible forms of CMA, only PEC problems are investigated. Mesh files are provided as input to the CM solvers to isolate the effect of different numerical schemes, rather than meshing strategies. With specific definitions for the impedance matrix calculations and solvers for the generalized eigenvalue equation, the following achievements were made through this joint work: a) A repository that includes numerical solutions of the three benchmark problems was developed, b) A suite of benchmark problems were cross-validated through collaborative efforts, c) A summary of the CMA results and their comparisons are provided in this paper.

II. CM BENCHMARK PROBLEMS

The three defined CM benchmark problems represent a certain class of problems that were previously solved and which are known to pose certain computational challenges. An indication of the accuracy of the CM computation can be obtained through comparing the numerical results of the independently developed CM solvers. To ensure that the requested parameter settings are sufficient to provide similar results, the robustness of these solvers is also studied through the independent use of the same solver (e.g., Altair FEKO) by more than one party. The verifications performed in this paper are based on consistency checks of the CMA results provided by 10 contributing parties.

A. Benchmark Problem 1: Rectangular PEC Plate

As shown in Fig. 1(a), the dimensions of the rectangular PEC plate are 0.1×0.04 m^2. The frequency range of interest should at least cover the resonant frequencies of the first four modes. Hence, based on previous CMA, the frequency range of 1-5 GHz is chosen. A frequency step of 0.1 GHz is defined to balance computational burden and possible investigation of frequency variation in modal quantities. The provided mesh is obtained from Altair FEKO by setting the average mesh density to 0.004 m (λ_0/15 @ 5 GHz). The number of triangles is 668. Unlike conventional scattering analysis, where a mesh density of λ_0/10-λ_0/8 is often sufficient, the finer mesh density here is to help model the more rapidly changing modal currents in high order modes. Apart from the eigenvalues, the required outputs are modal quantities of the dominant modes (i.e., modes with the smallest absolute eigenvalues), defined as:

- Modal currents at 1.3 GHz and 2.8 GHz;
- Modal far-fields in cut planes $\varphi = 0°$ and 90°, at 1.3 GHz and 2.8 GHz.

B. Benchmark Problem 2: Circular Disk

The circular disk with radius 0.1 m is shown in Fig. 1(b). The mesh for this benchmark problem is obtained from Altair FEKO by setting the average mesh density to 0.0086 meter (λ_0/10 @ 3.5 GHz). The number of triangles is 1186. The chosen frequency range for the CMA is 0.5-3.5 GHz ($1.05 \leq ka \leq 7.33$), with a frequency step of 0.05 GHz. The required outputs for the dominant modes are defined as:

- Modal currents at 1.0 GHz and 1.5 GHz;
- Modal far-fields in cut planes $\varphi = 0°$ and 90°, at 1.0 GHz and 1.5 GHz.

C. Benchmark Problem 3: PEC Sphere

The PEC sphere with radius 0.2 m is shown in Fig. 1(c). The mesh for this benchmark problem is obtained from Altair FEKO by setting the average mesh density to 0.0167 meter (λ_0/15 @ 1.2 GHz). The number of triangles is 4892. The frequency range for the CMA is 0.2-1.2 GHz ($0.84 \leq ka \leq 5.03$), with a frequency step of 0.02 GHz. The required outputs of dominant modes are defined as:

- Modal currents at 640 MHz and 900 MHz;
- Modal far-fields in cut planes $\varphi = 0°$ and 90°, at 0.64 GHz and 0.9 GHz.

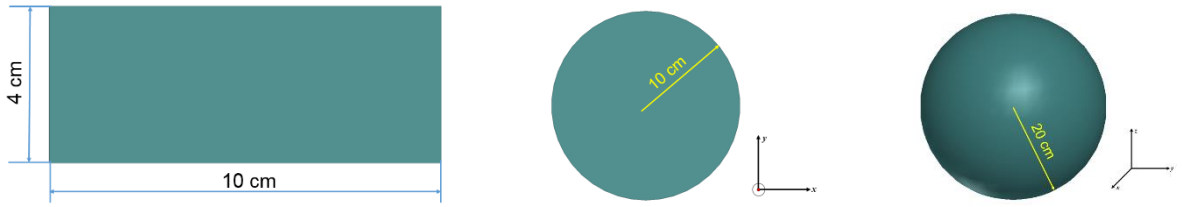

(a) (b) (c)

Fig. 1. Geometry of the benchmark problems. (a) Rectangular PEC plate; (b) PEC circular disk; (c) PEC sphere.

Table I. A List of Contributing Parties (named after abbreviated affiliations of this papers' co-authors) and CM Solver Properties

Contributing Parties	TCM Solver	Code for Impedance Matrix Filling	Solver for GEP	Contributing Parties	TCM Solver	Code for Impedance Matrix Filling	Solver for GEP
Altair FEKO	Altair FEKO	Altair FEKO	Altair FEKO	***METU***	In-house code	In-house method of moments (MoM) code	MATLAB eigs
BUAA	In-house code	Altair FEKO	MATLAB eigs	***NCSU***	In-house code	In-house MoM code	MATLAB eigs
CTU	In-house code	AToM code[13]	MATLAB eigs	***UNIPI***	Altair FEKO	Altair FEKO	Altair FEKO
LUH	In-house code	Modified Makarov code	MATLAB eigs	***UESTC***	In-house code	A-UEST (Accurate Universal EM Simulation Tool)	IRAM in ARPACK
LUND	In-house code	Makarov code	IRAM in Matlab	***WIPL-D***	WIPL-D	WIPL-D 3D MoM Solver	LAPACK routines

III. BENCHMARK RESULTS

There are 10 contributing parties from both universities or companies in this work (see Table I). Both in-house and commercial CM solvers are represented. In order to provide with reliable benchmarking results through this collaborative work, the contributing parties are requested to solve the three benchmark problems with these parameter settings at this stage:

- Types of basis functions: RWG basis function [14]
- Quadrature rule for surface integration on triangle elements: Gauss quadrature
- Number of Gauss quadrature points on each triangle element: 4
- Singularity treatment: Duffy transformation [15]
- Numerical solver for solving generalized eigenvalue equation (GEP): Implicitly Restarted Arnoldi Method (IRAM) in ARPACK[16]
- Numerical precision for calculations: double precision

However, some exceptions were made for several parties due to restrictions in their CM solvers, as described below:

1) Because WIPL-D uses quadrilateral mesh in their solver, the provided meshes were not used in their analysis. The number of quadrilateral patches for the rectangular PEC plate, circular disk, and sphere is 9, 256, and 942, respectively. High-order basis function is applied in discretizing the Electric Field Integral Equation (EFIE).

2) NCSU used a symmetric 9 × 9 uniform quadrature for integration on a triangle patch, and MATLAB routine *eigs* was employed for solving the GEP. Actually, the *eigs* routine is a wrapper of the ARPACK [16] for ease of implementation in MATLAB.

3) METU also implemented MATLAB routine *eigs* for solving the GEP. The singular term in the free-space Green's function is extracted using the method in [17] and the numerical integration on each triangle is taken using the 3-order Gaussian quadrature as presented in [18].

Cross-validations were performed for the eigenvalues as well as for modal currents and far-fields. The agreement achieved in the eigenvalues is generally satisfactory, except for some discrepancies in high frequencies. The modal currents and far-fields provided by the 10 groups appear to be somewhat different, but this was attributed to different plotting formats (e.g., type of colormap). The modal current figures provided by LUH are shown in the following results, as they are well suited for illustrating the behavior of modal currents. The modal currents and far-fields provided by all 10 contributing parties are available on the TCM SIG website [12].

A. Benchmark Problem 1: Rectangular PEC Plate

Fig. 2 presents the eigenvalues of the first six modes obtained from the 10 independent contributing parties. It is noted that $|\lambda|$ is used in the left panel of Fig. 2(a), instead of λ, when there are negative eigenvalues. The same plotting scheme is employed throughout this paper to clearly show the minor differences among the results from the 10 parties. In Figs. 2, the right panels give an enlarged view of the frequency range with relatively large discrepancies. As can be seen, the eigenvalues agree well with each other in the frequency range of 1.0-3.5 GHz for all of the six modes, whereas discrepancies (< 1 dB) appear in the range of 3.5-5.0 GHz for the 1st mode. The discrepancies become large in 3.5-5.0 GHz for the 2nd, 4th, and 5th modes. This is because the eigenvalues in the range of 3.5-5.0 GHz have very small absolute values. Therefore, the disagreement is mainly caused by the numerical errors in the impedance matrix calculation and the errors in solving the GEPs. Fig. 3 shows the modal currents of the dominant mode at 1.3 GHz and 2.8 GHz provided by 10 contributing parts, where yellow (or red) denotes maximum current and blue is the minimum current. It clearly shows a resonant behavior in the first two modes. In spite of the plotting formats, the modal current distributions are generally in good agreement with each other. Fig. 4 shows the comparison of the modal far-fields of the dominant mode at 1.3 GHz and 2.8 GHz. As we can see, the minima fields and maxima fields exist at the same angle in the patterns shown in Fig. 4(a), (b), and (d). The discrepancies appear mainly in the slopes and null depths. However, there are obvious angle shifts in the maximum radiation direction in Fig. 4(c).

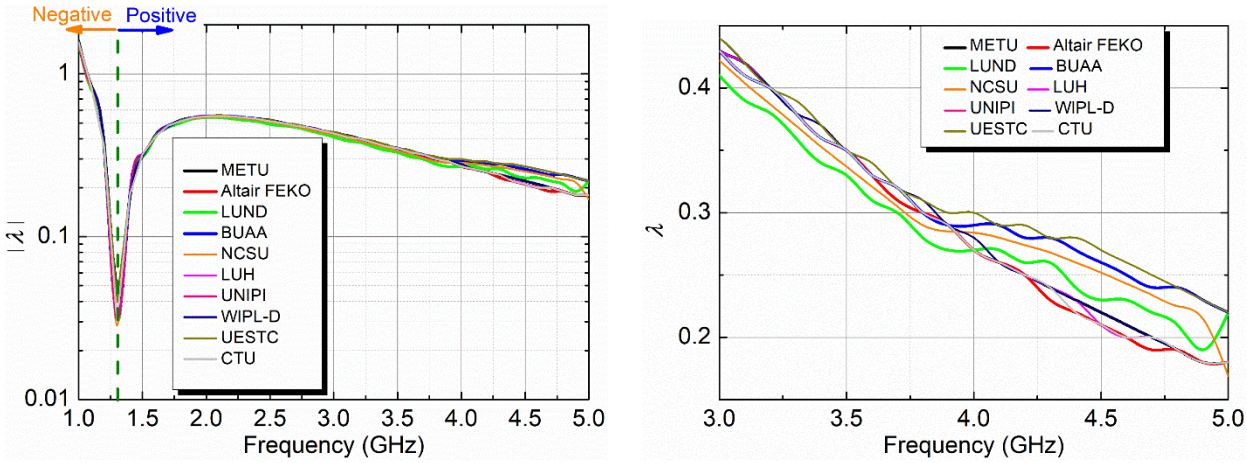

(a) 1st mode

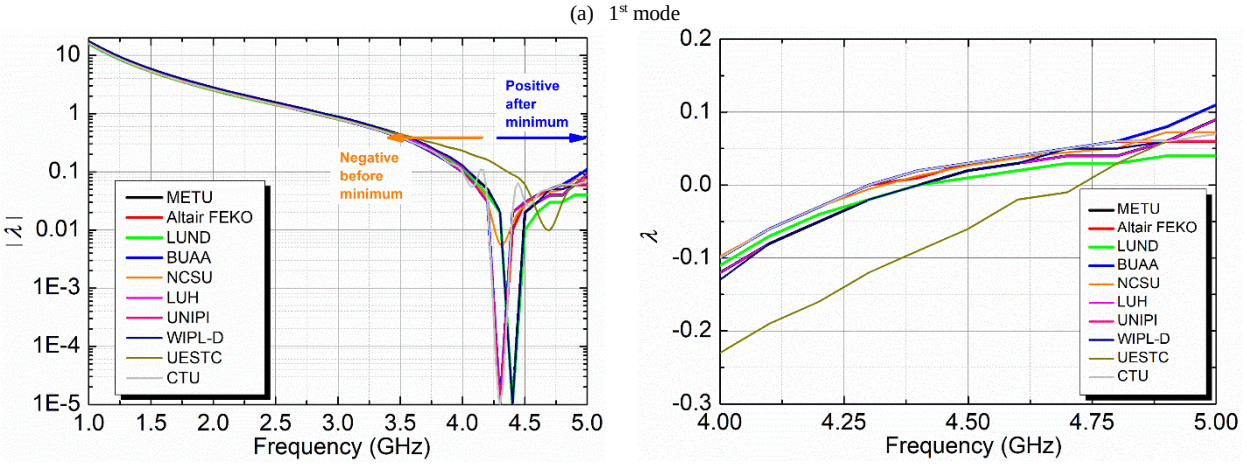

(b) 2nd mode

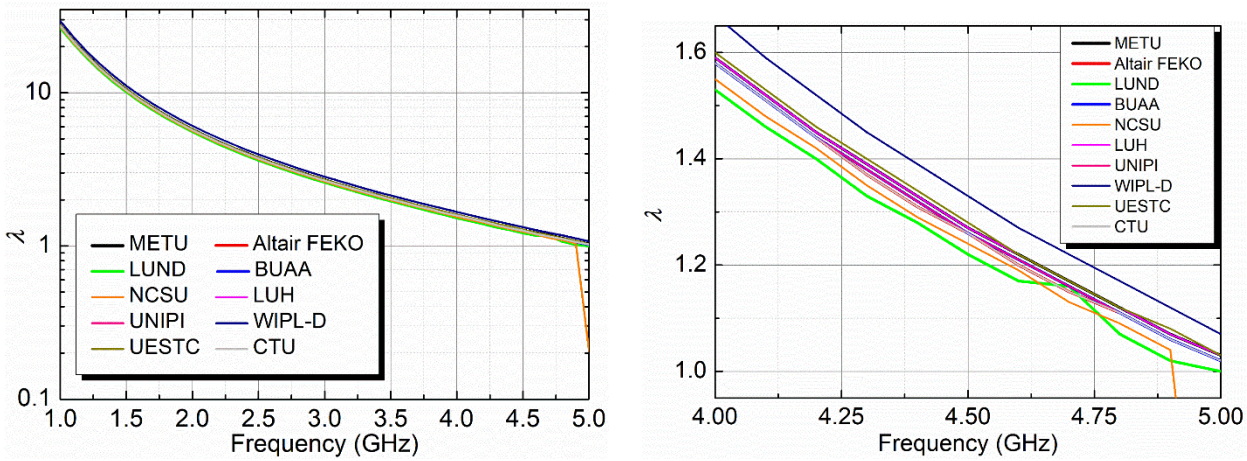

(c) 3rd mode

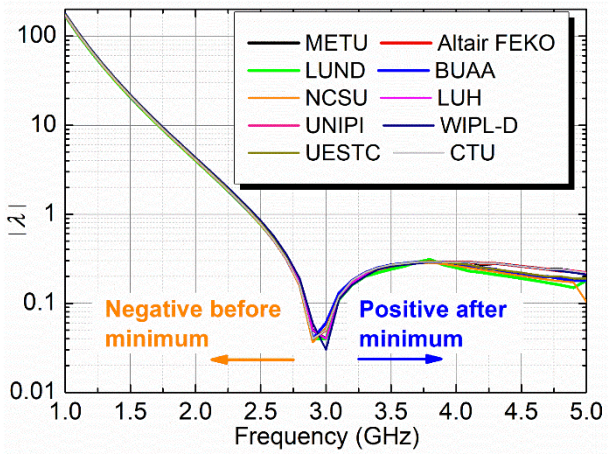

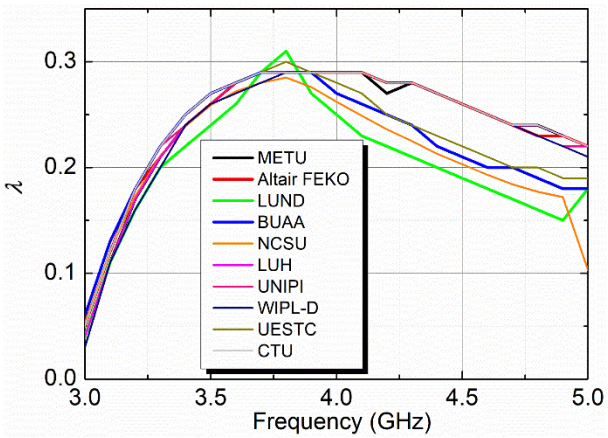

(d) 4th mode

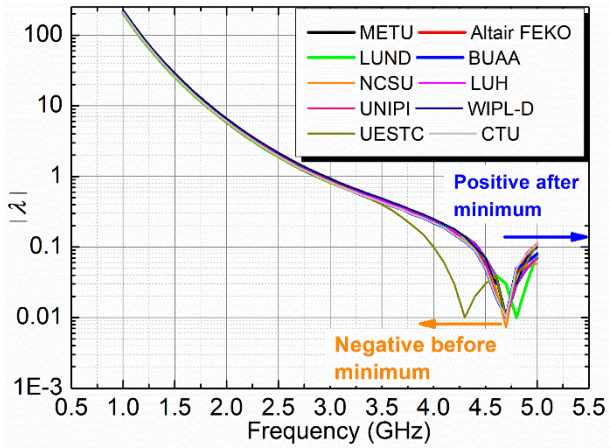

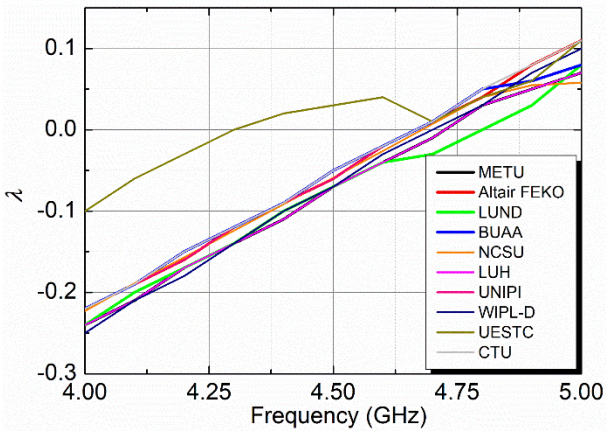

(e) 5th mode

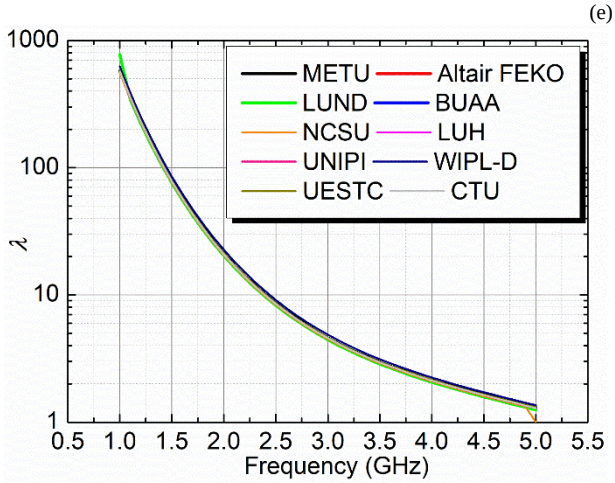

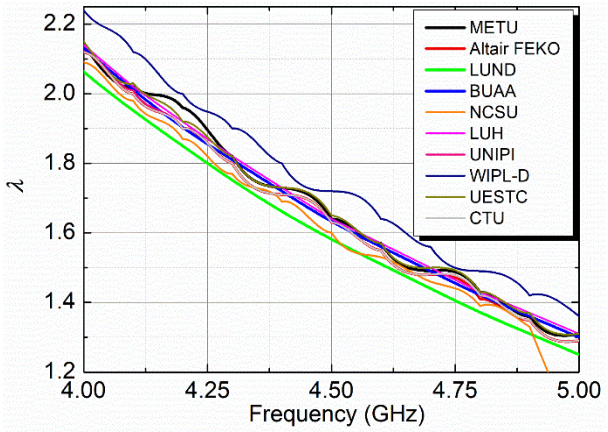

(f) 6th mode

Fig. 2. Comparison of the eigenvalues for the first 6 modes in problem 1.

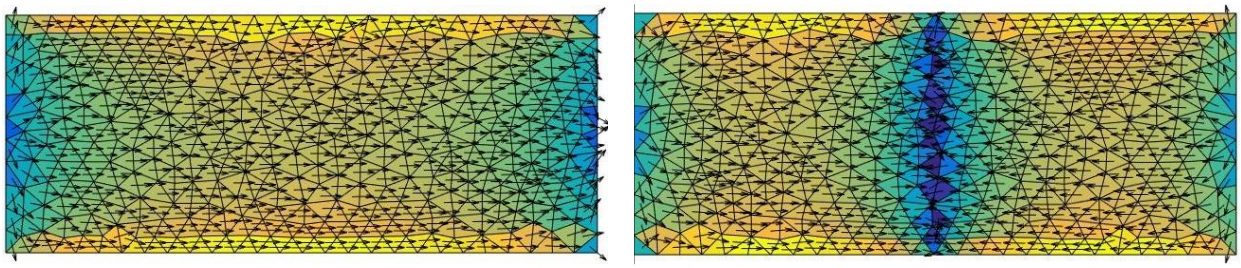

(a) METU

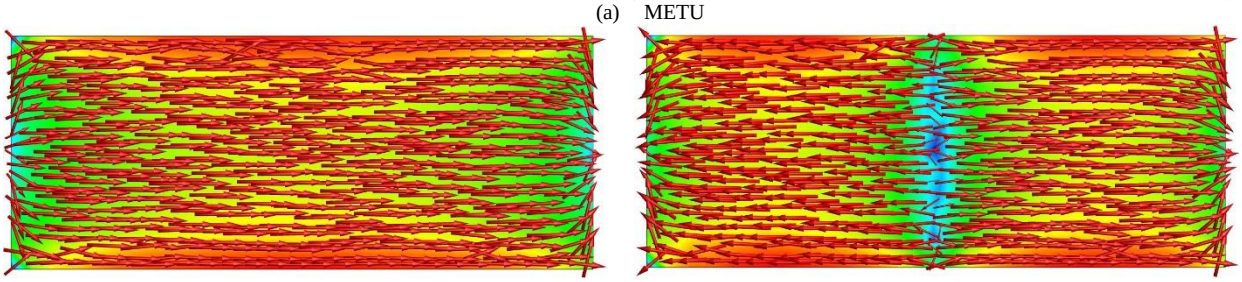

(b) Altair FEKO

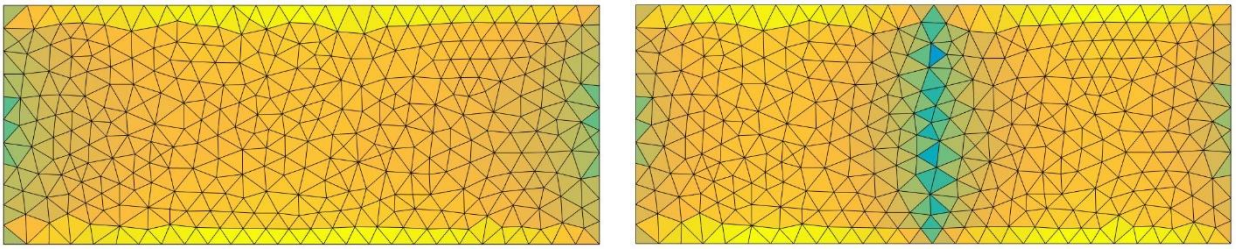

(c) LUND

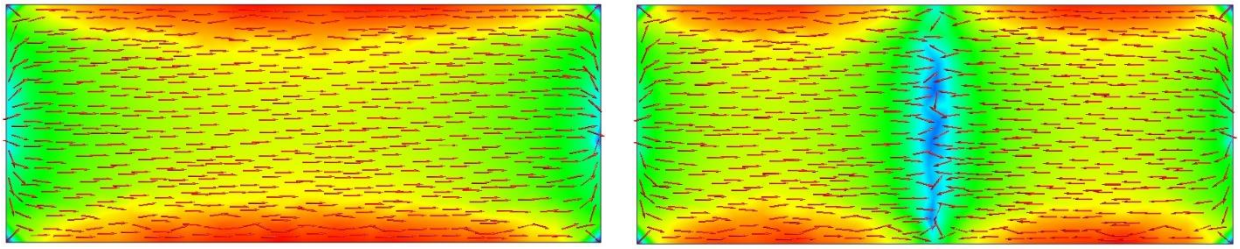

(d) BUAA

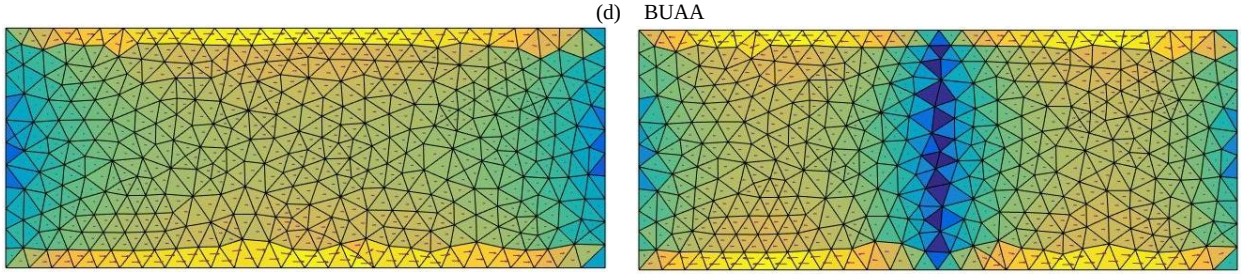

(e) NCSU

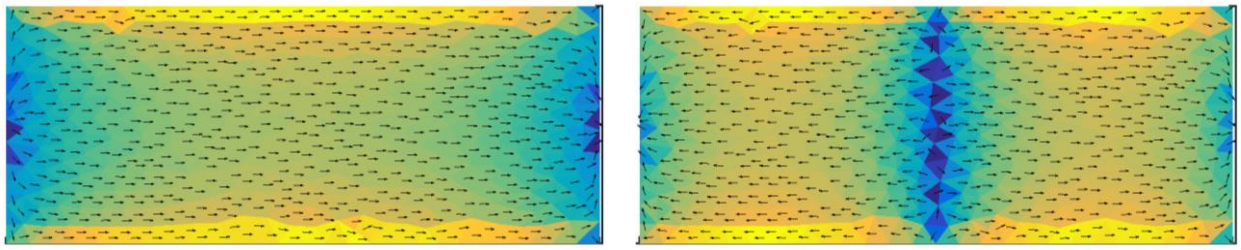

(f) LUH

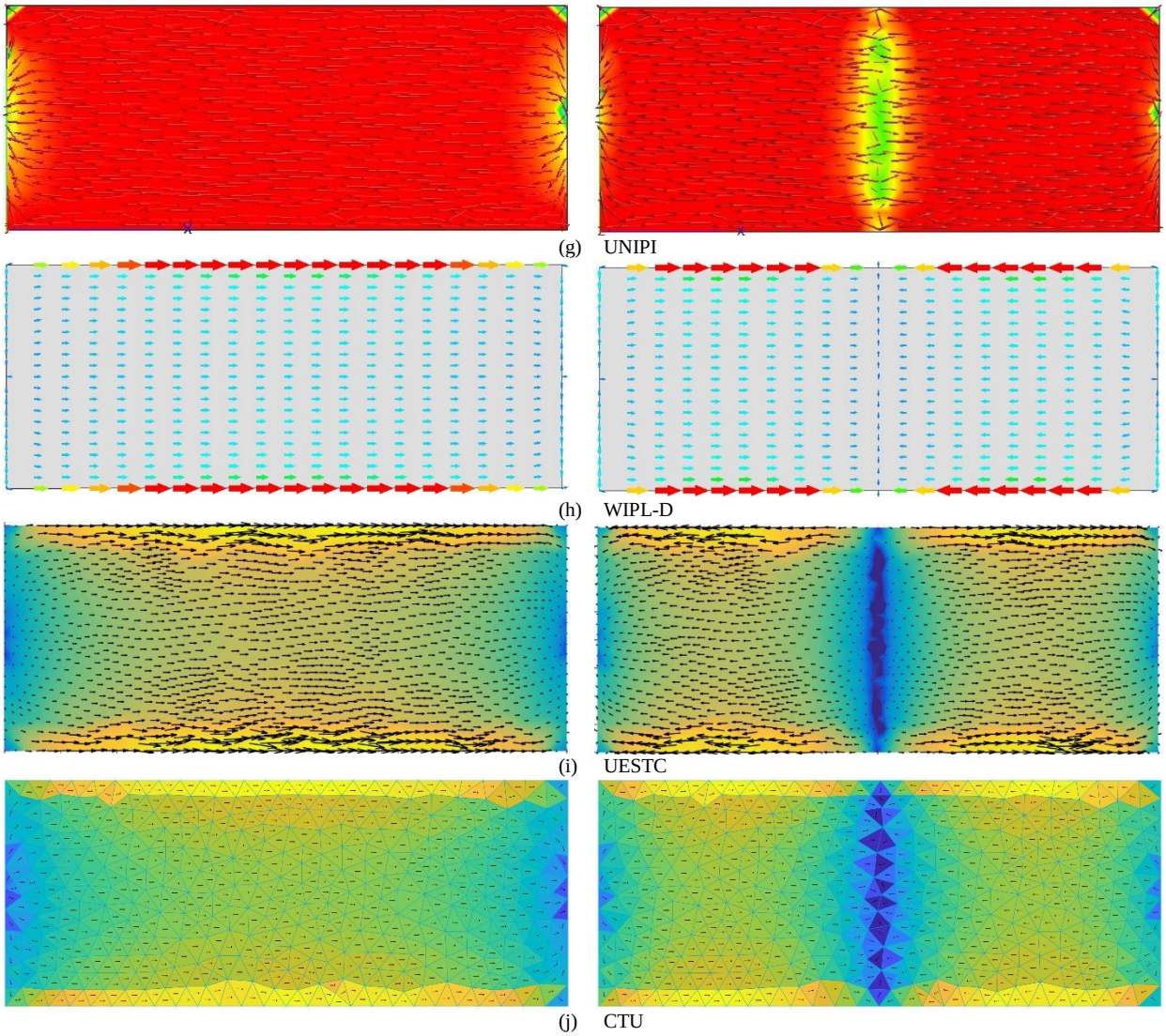

Fig. 3. Dominant modal currents at 1.3 GHz (left) and 2.8 GHz (right).

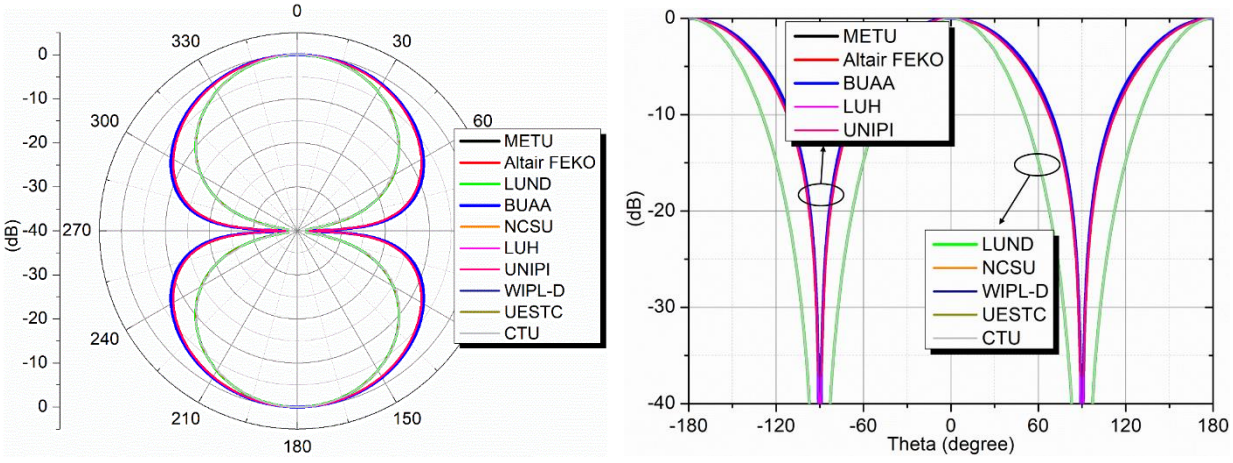

(a) φ = 0° @ 1.3 GHz

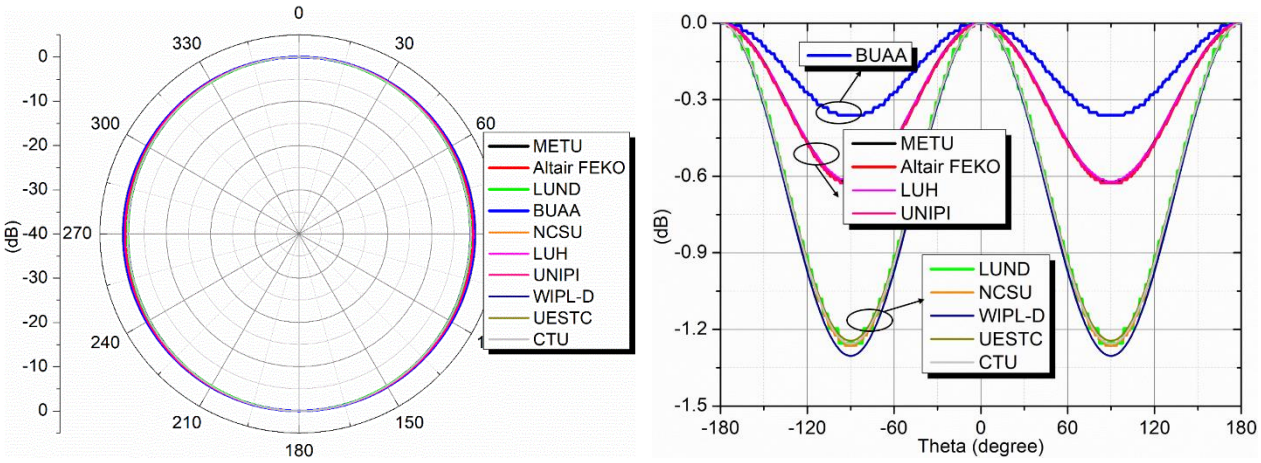

(b) φ = 90° @ 1.3 GHz

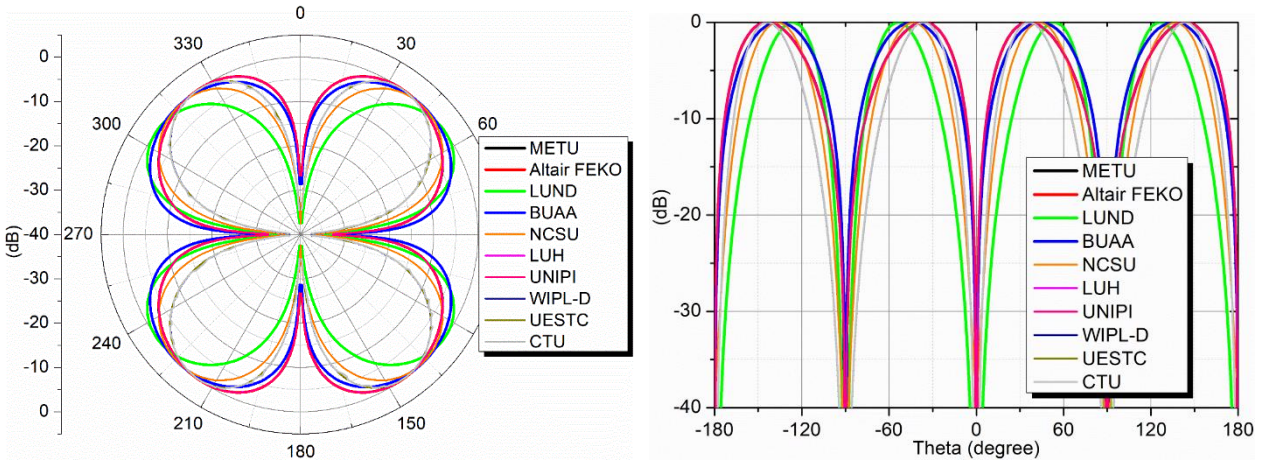

(c) φ = 0° @ 2.8 GHz

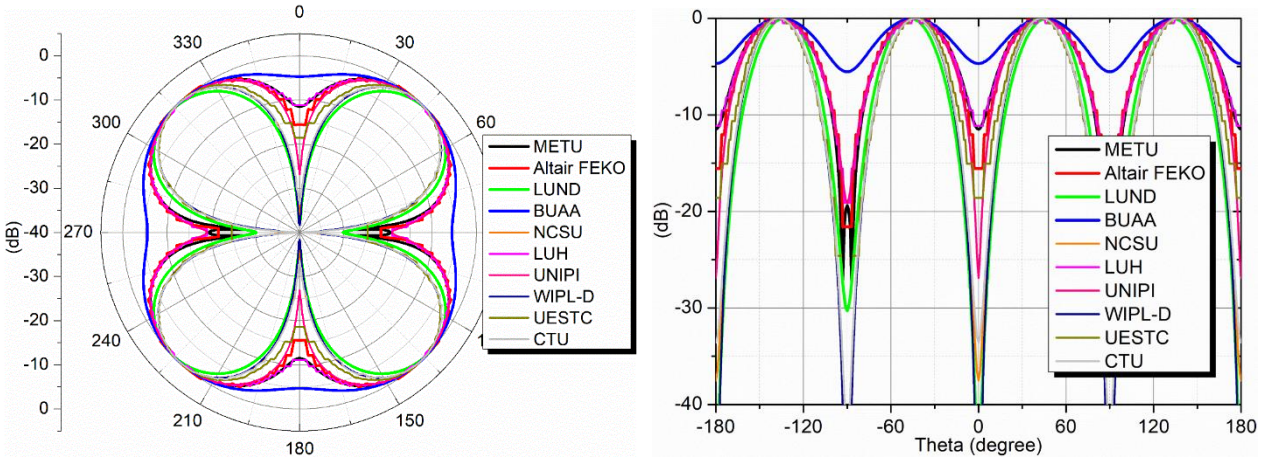

(d) φ = 90° @ 2.8 GHz

Fig. 4. Comparison of the modal far-fields in cut planes φ = 0° and 90° at 1.3 GHz and 2.8 GHz.

B. Benchmark Problem 2: Circular Disk

Owing to the rotational symmetry of the circular disk, several modes have the exactly same eigenvalues but rotational symmetric modal currents and far-fields. Hence, modes with the same eigenvalues but rotational symmetric modal current distributions are considered as the same mode. Fig. 5 compares the eigenvalues of the first four modes obtained from the 10 contributing parties. As it can be seen, eigenvalues solved by the 10 parties are in good agreement in the frequency range of 0.5-1.5 GHz for the four modes.

However, the values appear very different in the range of 1.5-3.5 GHz, where the eigenvalues have very small absolute values (< 0.01). This differences are attributed to numerical errors affecting each step of the CMA. Fig. 6 gives the modal currents of the dominant mode at 1.0 GHz and 1.5 GHz. A good agreement is achieved except the modal current at 1.5 GHz provided by WIPL-D. They are all flowed from one end to the opposite one, which behaves like a 0.5 λ dipole. Owing to the discrepancies of the angles between the preset axis and modal currents, the modal far-fields in cut planes $\varphi = 0°$ and 90° are quite different (except for the results from WIPL-D---the navy line shown in Fig. 7(c) and (d)---which is totally mismatch with others).

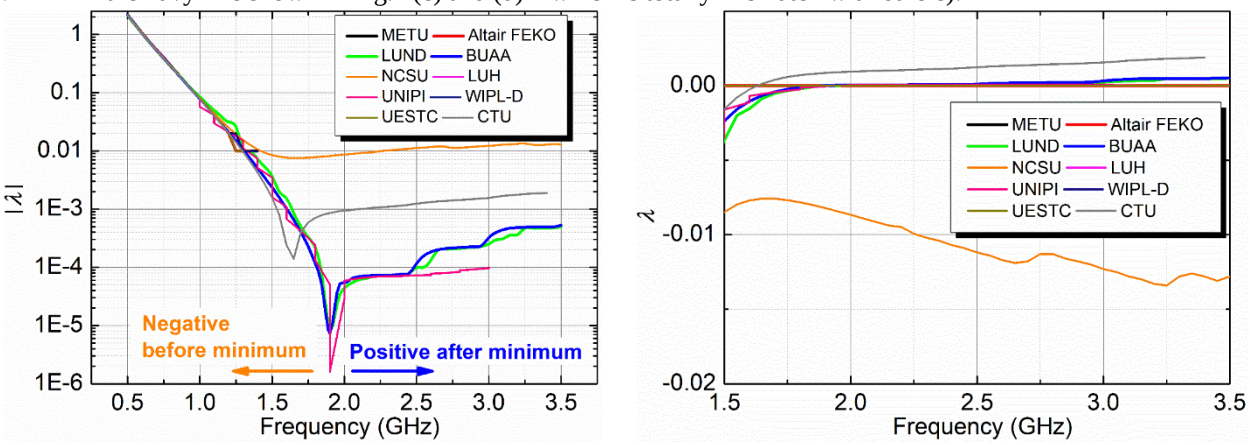

(a) 1st mode

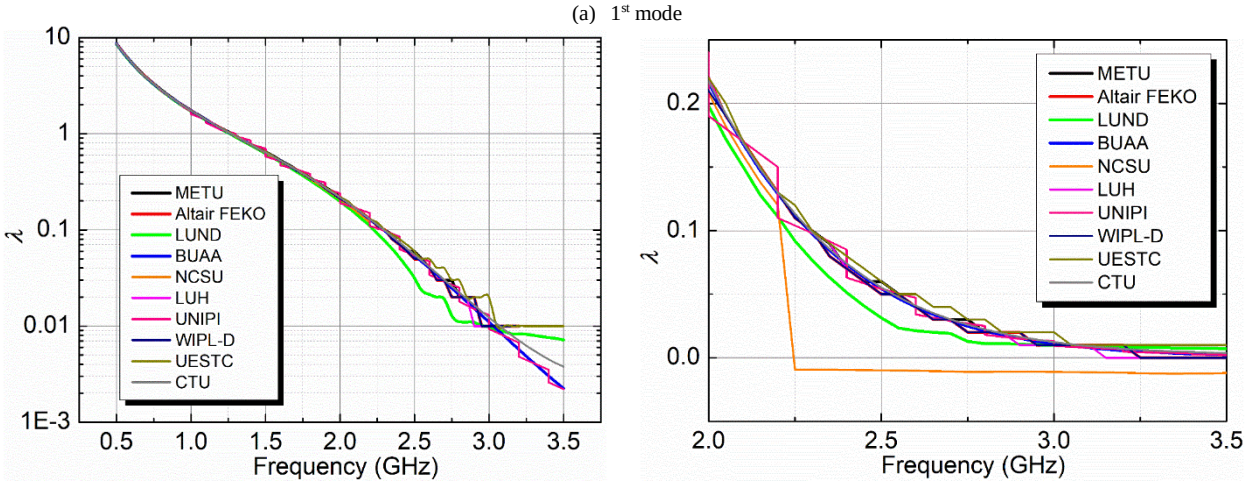

(b) 2nd mode

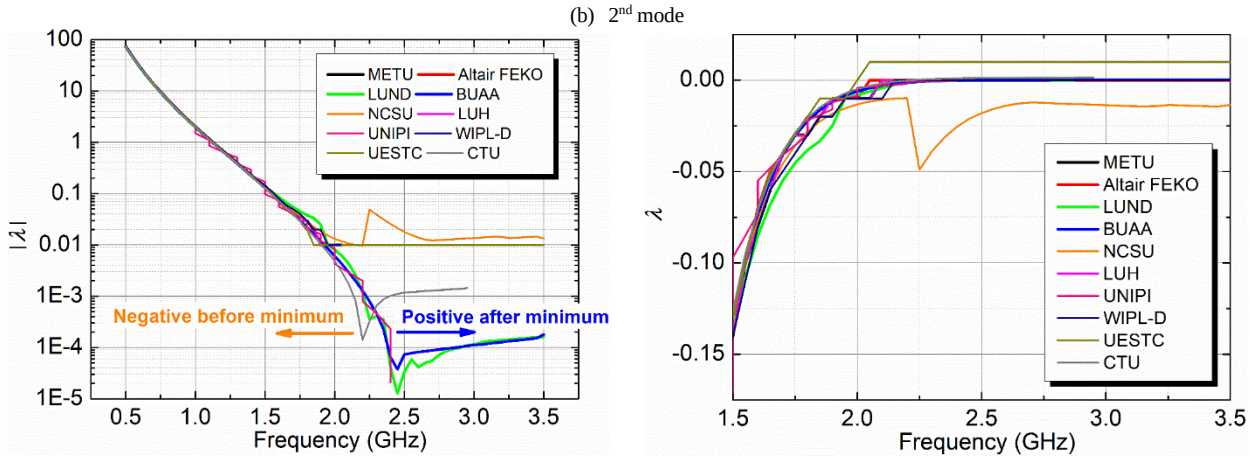

(c) 3rd mode

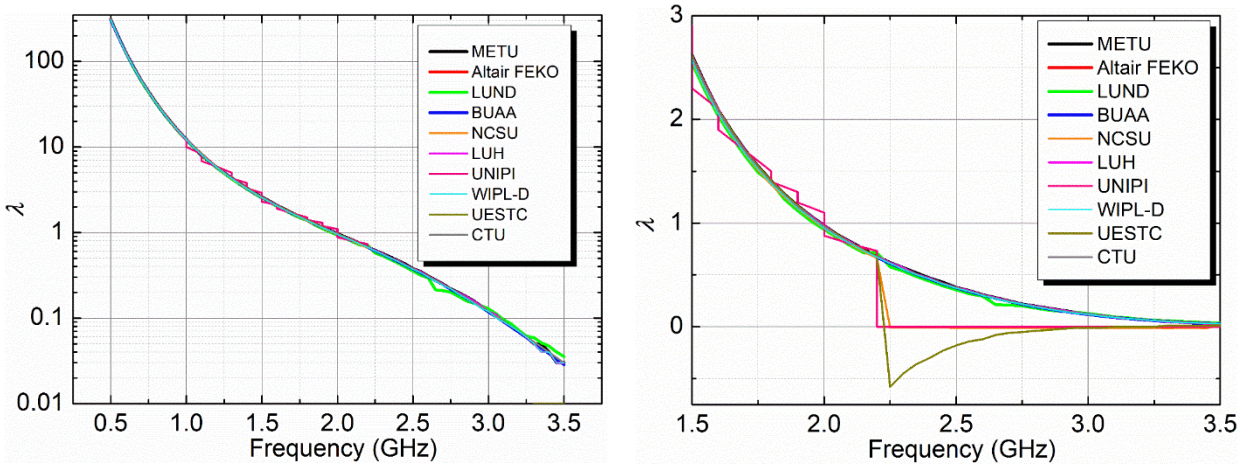

(d) 4th mode

Fig. 5. Comparison of the eigenvalues for the first 4 modes in problem 2.

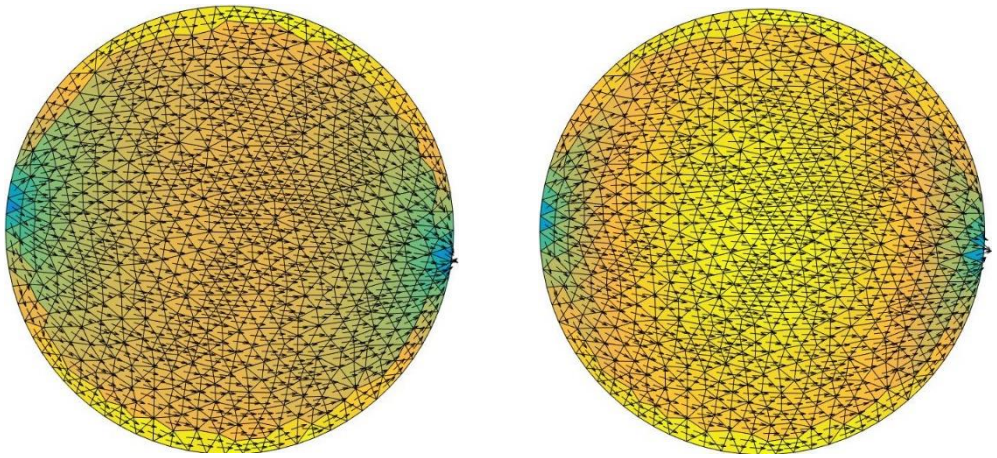

(a) METU

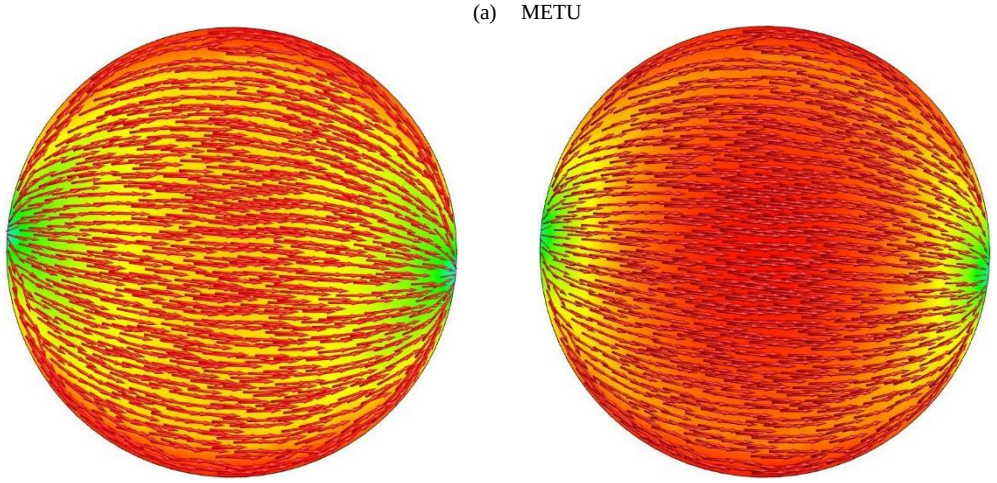

(b) Altair FEKO

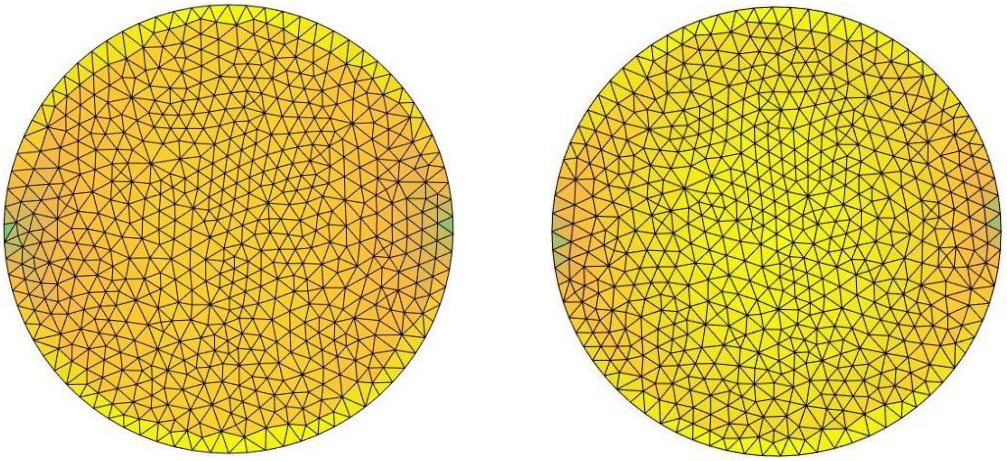

(c) LUND

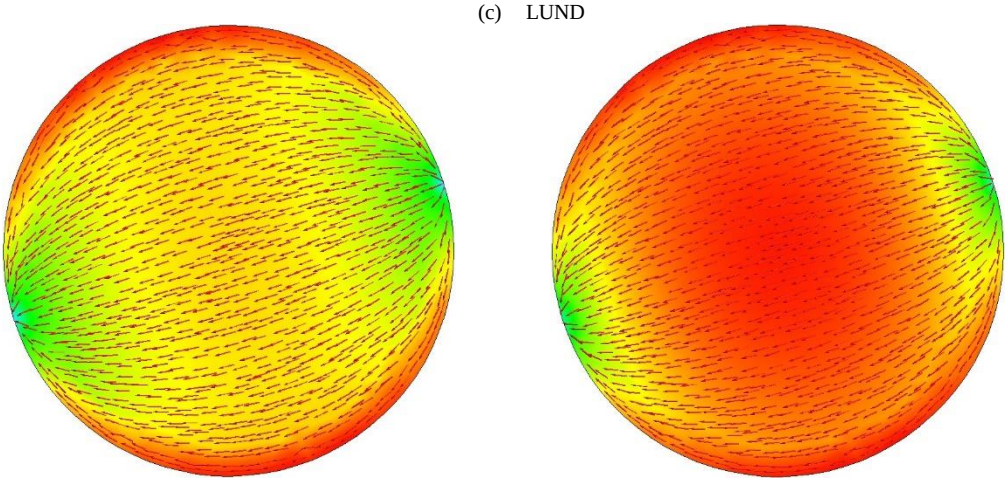

(d) BUAA

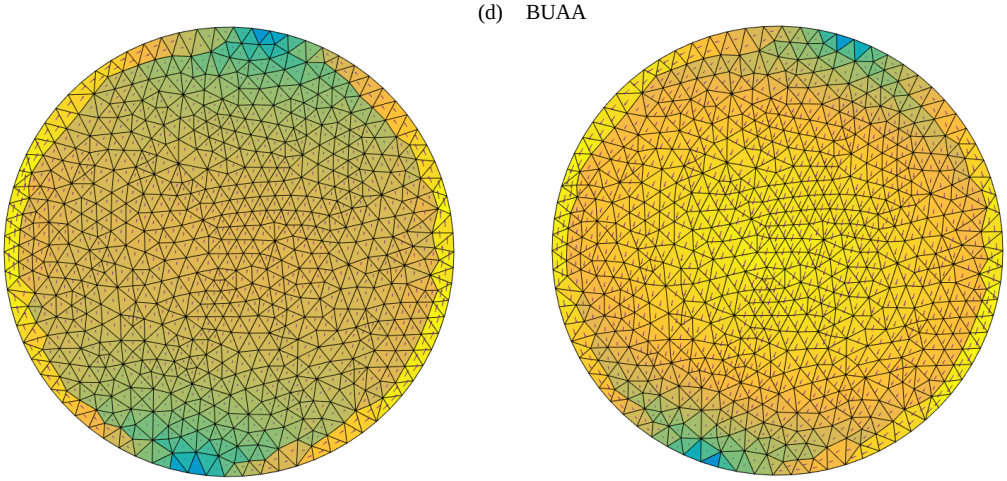

(e) NCSU

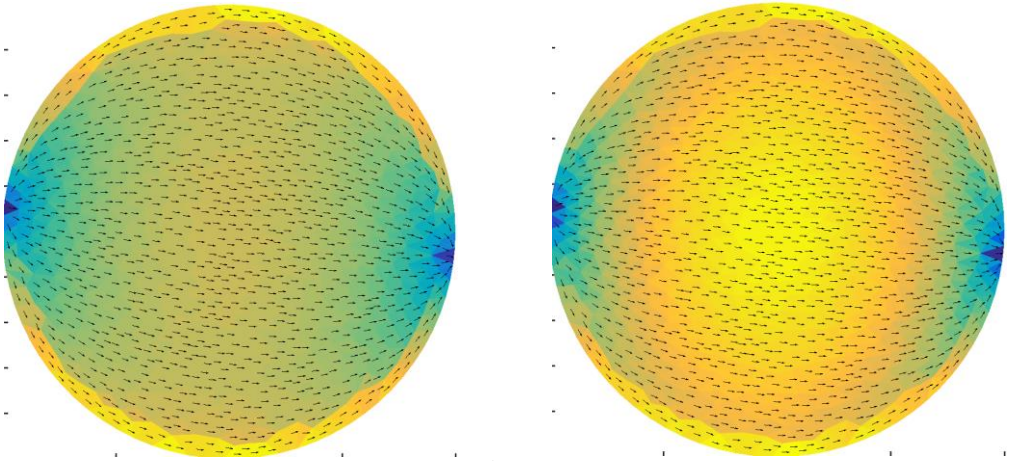

(f) LUH

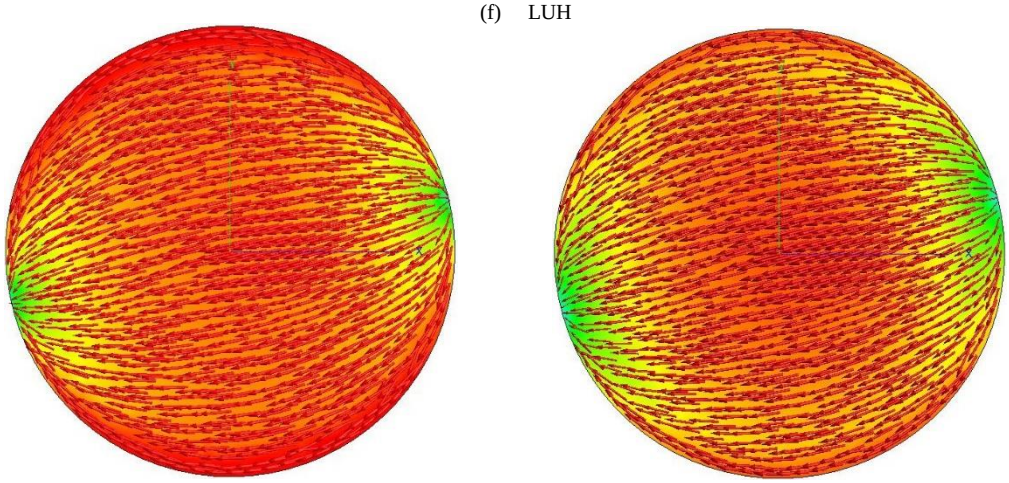

(g) UNIPI

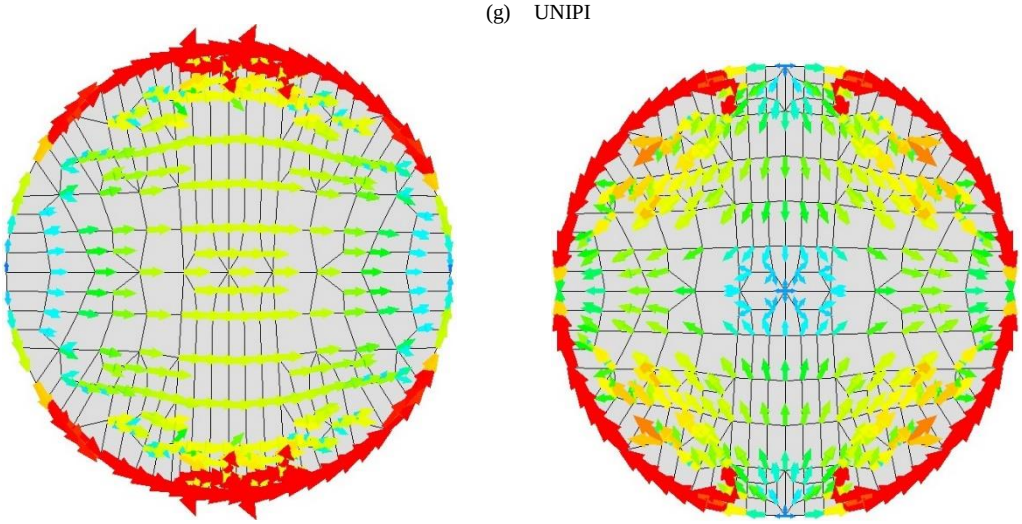

(h) WIPL-D

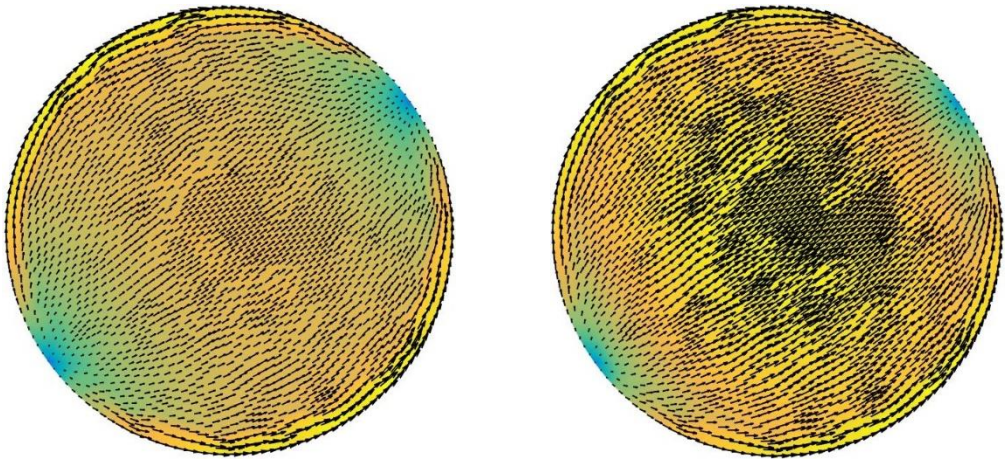

(i) UESTC

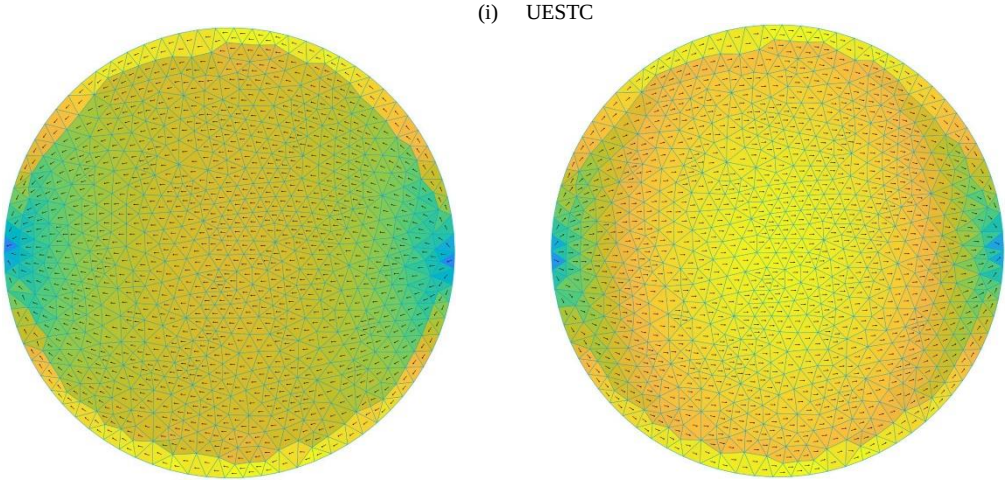

(j) CTU

Fig. 6. Dominant modal currents at 1.0 GHz (left) and 1.5 GHz (right).

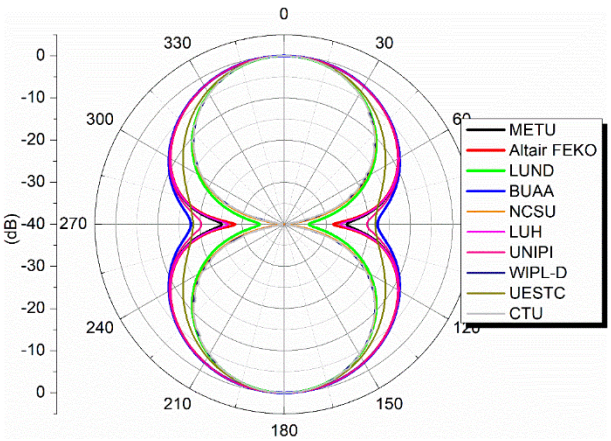

(a) φ = 0° @ 1.0 GHz

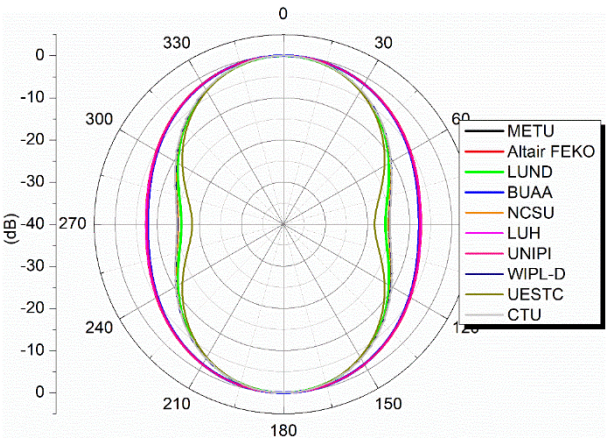

(b) φ = 90° @ 1.0 GHz

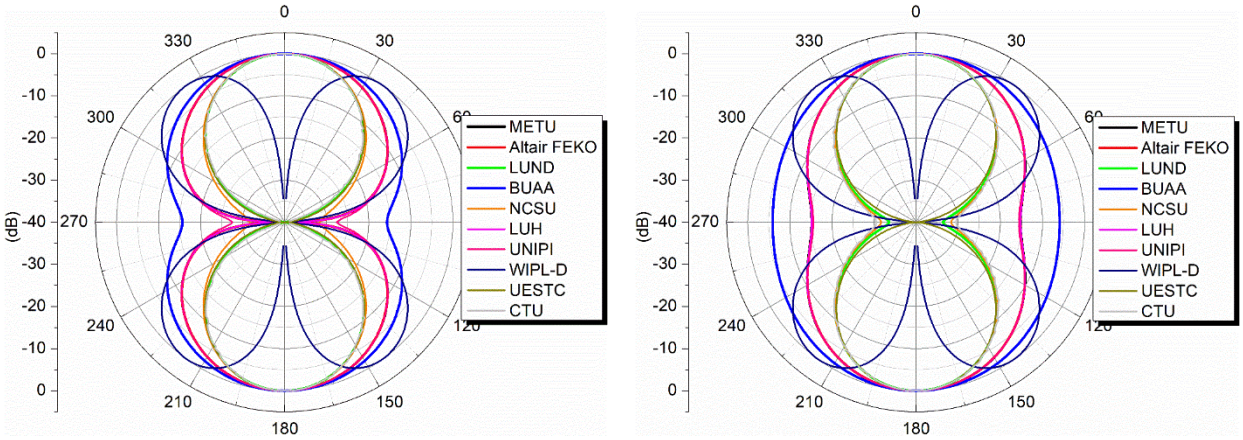

(c) φ = 0° @ 1.5 GHz (d) φ = 90° @ 1.5 GHz

Fig. 7. Comparison of the modal far-fields in cut planes φ = 0° and 90°at 1.0 GHz and 1.5 GHz

C. Benchmark Problem 3: PEC Sphere

As in problem 2, due to symmetry in the PEC sphere, there are several modes having the same eigenvalue but rotational symmetric modal currents and far-fields. Hence, modes with the same eigenvalues but rotational symmetric modal current distributions are considered as the same mode. In addition, it is found that the number of modes extracted in a CM solver for a single run will make the final eigenvalue plot look quite different. If the CMA strictly follows the recommendations given in the second call-for-contribution for this benchmark development [12], the first 12 modes at each frequency should be solved in a single run. The eigenvalues obtained in this way are shown in Fig. 8(a). Alternatively, if 20 or more modes were extracted (per frequency) in the CMA, the eigenvalues should be similar to those in Fig. 8(b). However, if the eigenvalues of Fig. 8(a) were superimposed on those of Fig. 8(b), the eigenvalues of a particular set of modes agree well across the whole frequency range. The modal currents of the dominant modes at 640 MHz and 900 MHz are shown in Fig. 9. As can be seen, two nulls appear in the modal current at 640 MHz and six nulls appear in the modal current at 900 MHz. Fig. 10 shows the comparison of the modal far-fields in cut planes φ = 0° and 90° at 640 MHz. Due to the same reason discussed in problem 2, great differences exist in both cut planes. Therefore, the modal far-fields at 900 MHz are not presented.

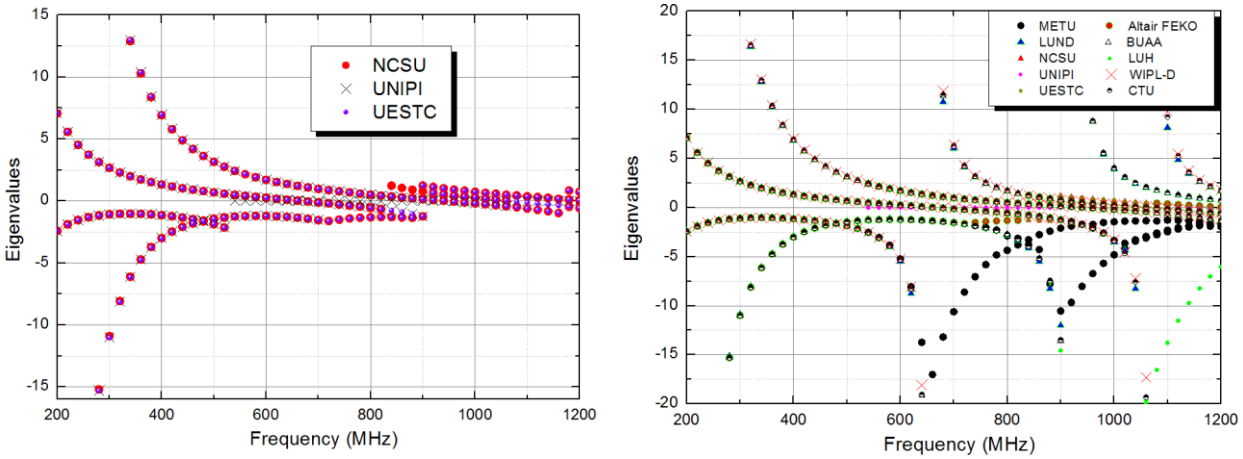

(a) (b)

Fig. 8. Eigenvalues of benchmark problem 3. (a) Case 1: 12 modes solved; (b) Case 2: More than 12 modes solved.

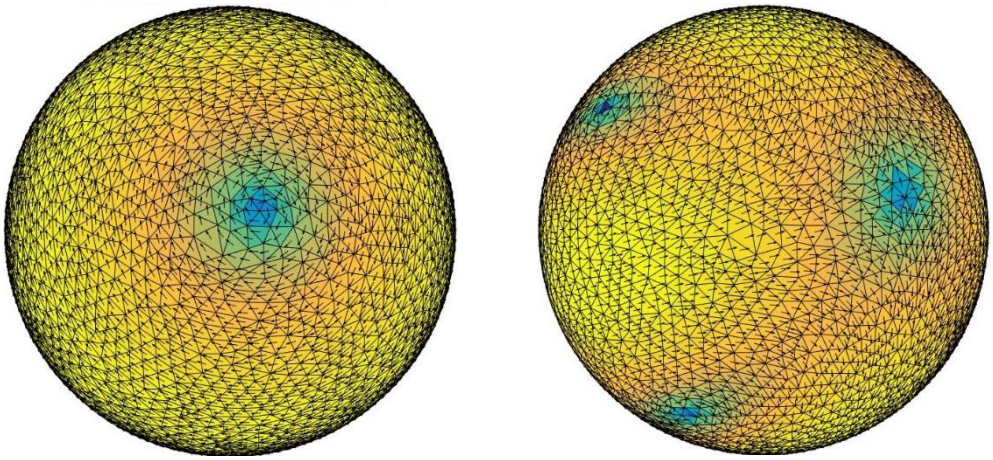

(a) METU

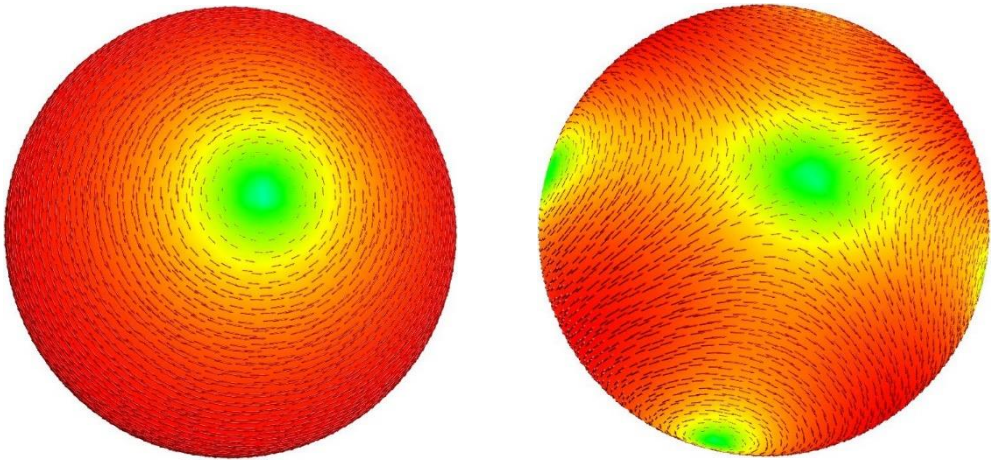

(b) Altair FEKO

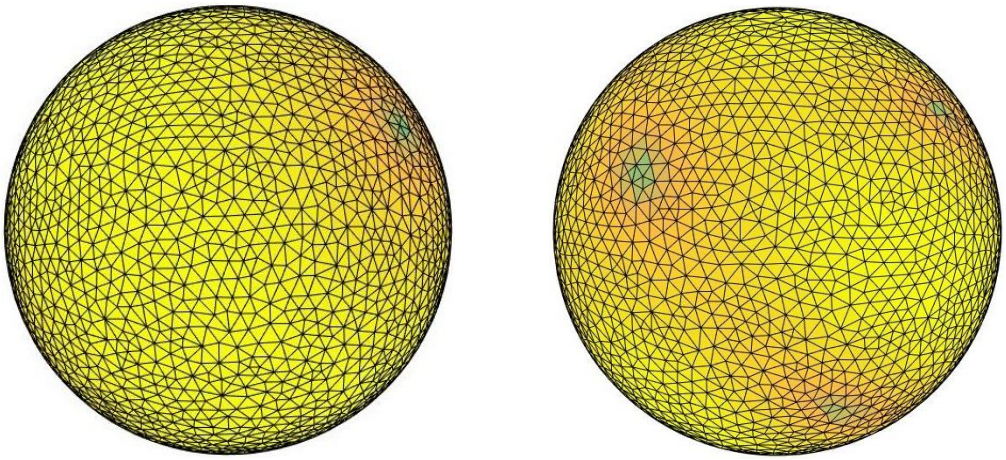

(c) LUND

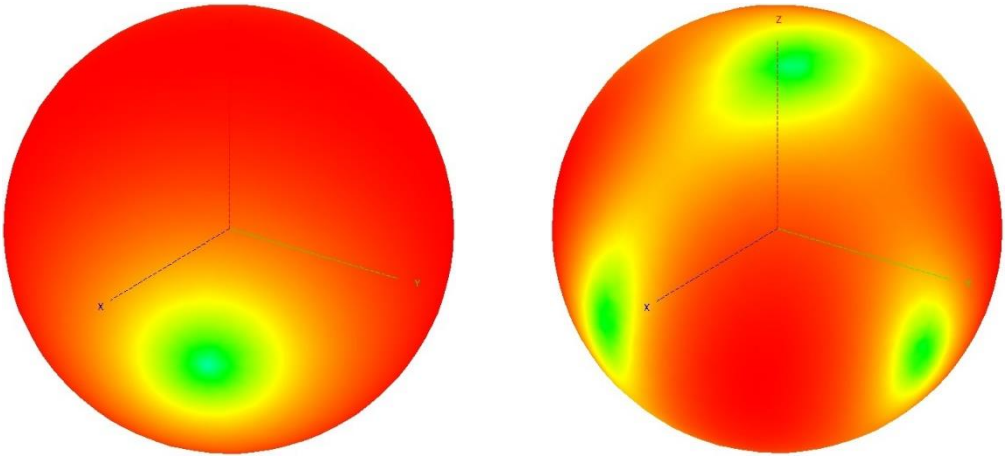

(d) BUAA

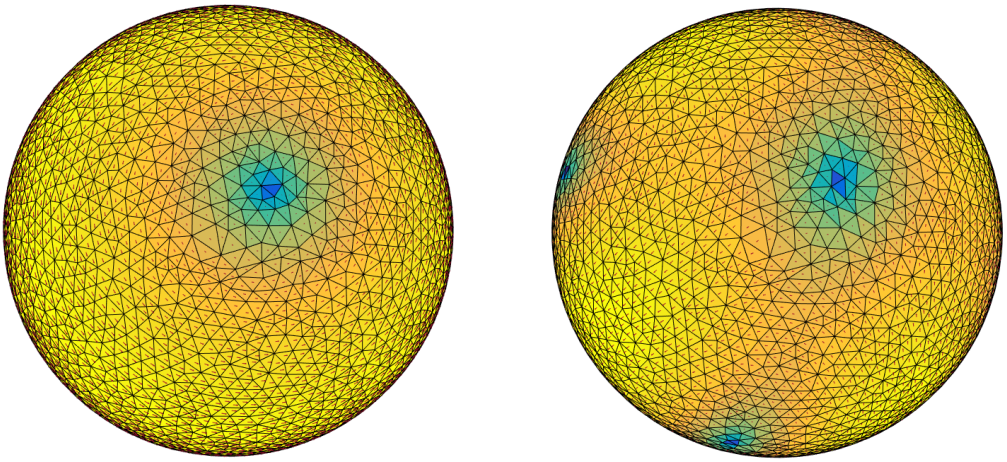

(e) NCSU

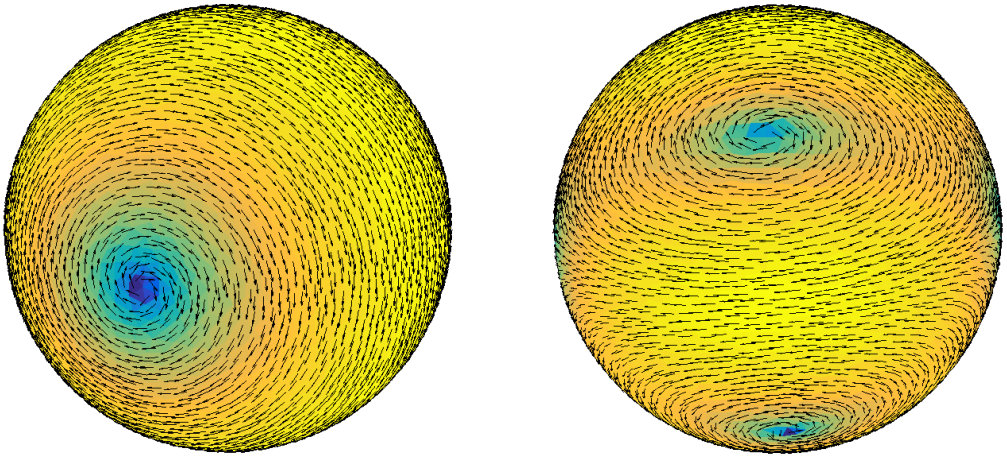

(f) LUH

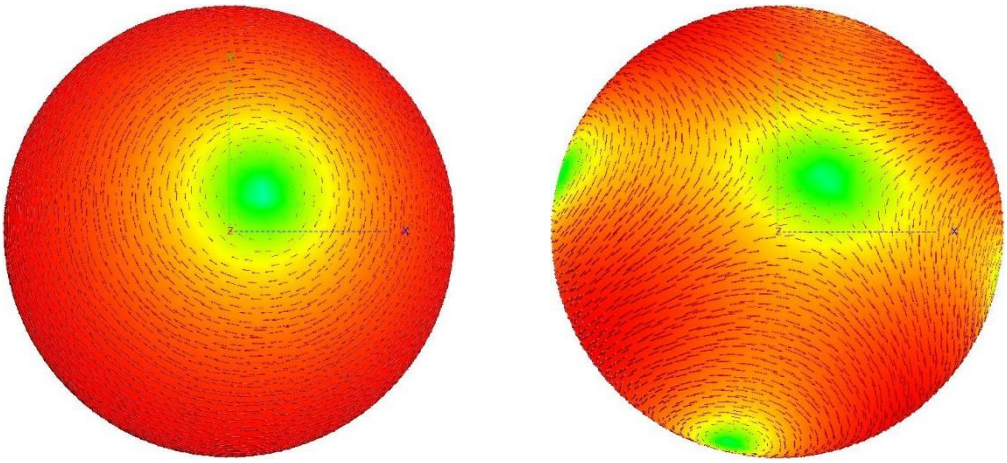

(g) UNIPI

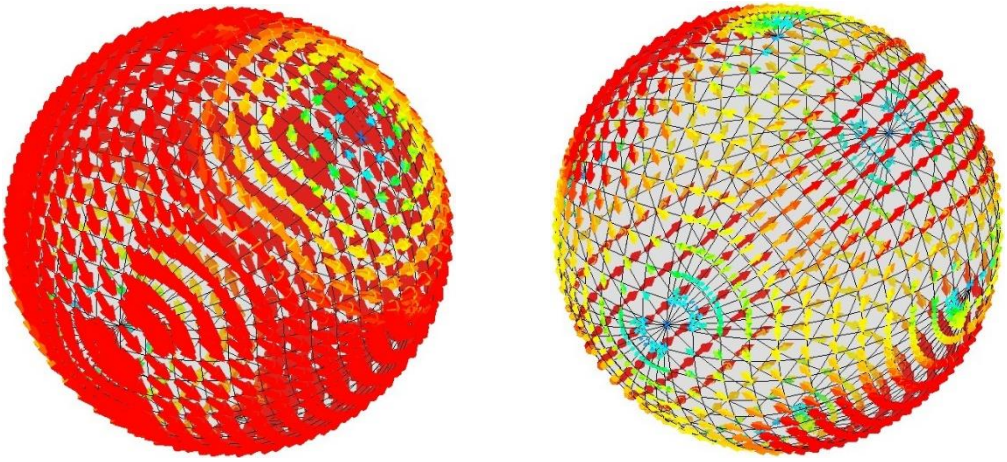

(h) WIPL-D

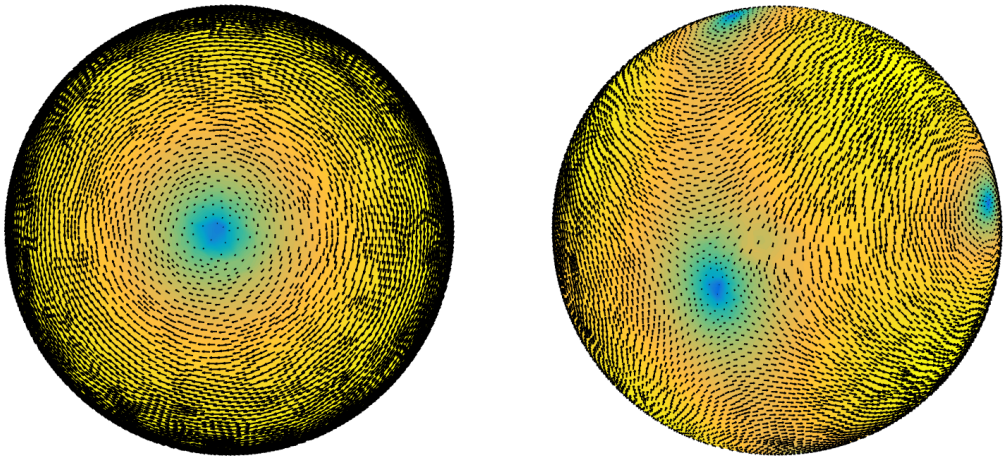

(i) UESTC

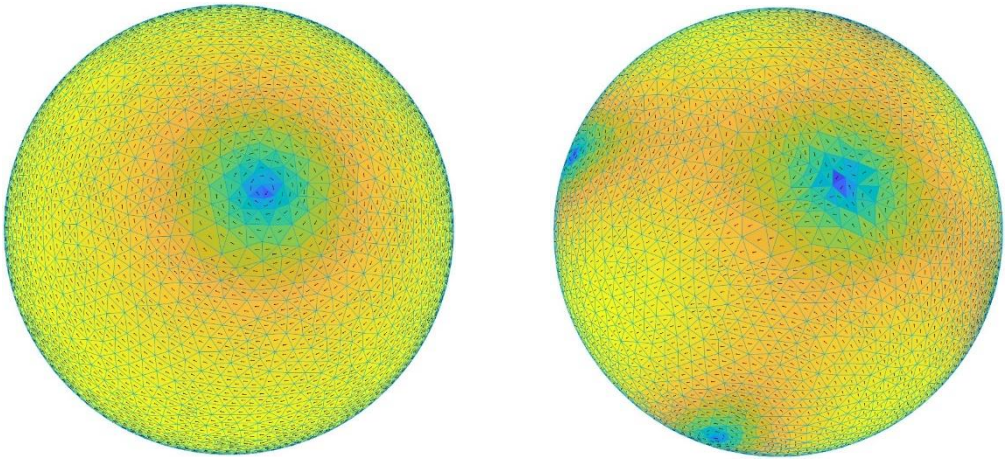

(j) CTU

Fig. 9. Dominant modal currents at 640 MHz (left) and 900 MHz. (right)

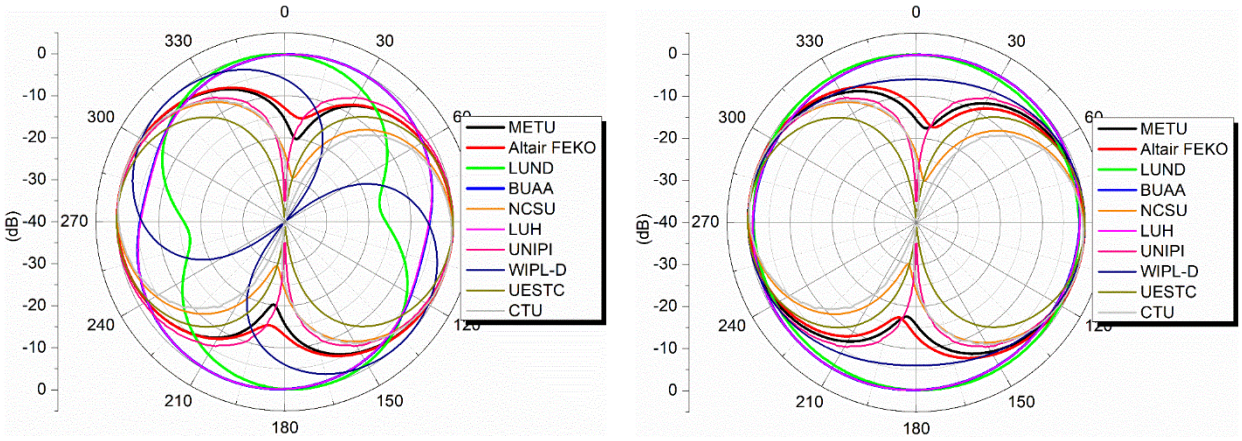

Fig. 10. Comparison of the modal far-fields in cut planes φ = 0° and 90°at 640 MHz.

IV. Conclusions and Futher Work

In this work, three CM benchmark problems and results from 10 contributing parties are presented. The provided meshes were used by all contributing parties except for WILP-D. However, mesh differences are not expected to be a major source of error as the three benchmark problems are all regular structures without any sharp edge. The complete CMA results for the three benchmark problems as produced by the 10 contributing parties are presented on the TCM SIG website [12] as a further reference. Although there are some discrepancies among the results, the eigenvalues and the modal currents from different parties generally agree well with one another. Nonetheless, further work should be carried out to provide more reliable benchmark results by enforcing more exact parameter settings for CMA. Readers are encouraged to respond to this paper and suggest additional problems that are suitable for benchmarking. We also encourage independent researchers to verify these results by performing direct comparisons.

References

[1] R. J. Garbacz, "Modal expansions for resonance scattering phenomena," *Proc. IEEE*, vol. 53, no. 8, pp. 856–864, Aug. 1965.

[2] R. F. Harrington and J. R. Mautz, "Theory of characteristic modes for conducting bodies," *IEEE Trans. Antennas Propag.*, vol. 19, no. 5, pp. 622–628, Sep. 1971.

[3] M. Cabedo-Fabres, E. Antonino-Daviu, A. Valero-Nogueira, M. F. Bataller, "The theory of characteristic modes revisited: A contribution to the design of antennas for modern applications," *IEEE Antennas Propag. Mag.*, vol. 49, no. 5, pp. 52–68, Oct. 2007.

[4] H. Li, Z. Miers, and B. K. Lau, "Design of orthogonal MIMO handset antennas based on characteristic mode manipulation at frequency bands below 1GHz," *IEEE Trans. Antennas Propag.*, vol.62, no.5, pp.2756–5766, May 2014

[5] Y. Chen, C.-F. Wang, "Electrically small UAV antenna design using characteristic modes," *IEEE Trans. Antennas Propag.*, vol. 62, no. 2, pp. 535–545, Feb. 2014.

[6] M. Vogel, G. Gampala, D. Ludick, et al., "Characteristic mode analysis: Putting physics back into simulation," *IEEE Antennas Propag. Mag.*, vol. 57, no. 2, pp. 307–317, Apr. 2015.

[7] E. Safin and D. Manteuffel, "Manipulation of characteristic wave modes by impedance loading," *IEEE Trans. Antennas Propag.*, vol. 63, no. 4, pp. 1756–1764, Apr. 2015.

[8] B. Yang and J. J. Adams, "Computing and visualizing the input parameters of arbitrary planar antennas via eigenfunctions," *IEEE Trans. on Antennas Propag.*, vol. 64, no. 7, pp. 2707–2718, Jul. 2016.

[9] A. Vasylchenko, Y. Schols, W. De Raedt, and G. A. E. Vandenbosch, "Quality assessment of computational techniques and software tools for planar-antenna analysis," *IEEE Antennas Propag. Mag*., vol. 51, no. 1, pp. 23-38, Feb. 2009.

[10] D. B. Davidson, *Computational Electromagnetics for RF and Microwave Engineering*, 2nd Ed, Cambridge University Press, 2010.

[11] M. Capek, V. Losenicky, L. Jelinek, and M. Gustafsson, "Validating the characteristic modes solvers," *IEEE Trans. Antennas Propag.*, vol. 65, no. 8, pp. 4134–4145, Aug. 2017.

[12] TCM SIG Website: http://www.characteristicmodes.org/

[13] Antenna Toolboxs for Matlab (AToM), Czech Technical University in Prague, 2017.

[14] S. M. Rao, D. R. Wilton, and A. W. Glisson, "Electromagnetic scattering by surfaces of arbitrary shape," *IEEE Trans. Antennas Propag*., vol. 30, no. 5, pp. 409–418, May 1982.

[15] M. G. Duffy, "Quadrature over a pyramid or cube of integrands with a singularity at a vertex," *SIAM J. Numer. Anal.*, vol. 19,no. 6, pp. 1260–1262, 1982.

[16] http://www.caam.rice.edu/software/ARPACK/

[17] D. Wilton, et al., "Potential integrals for uniform and linear source distributions on polygonal and polyhedral domains," *IEEE Trans. Antennas Propag*., vol. 32, no. 3, pp. 276–281, Mar. 1984.

[18] D. A. Dunavant, "High degree efficient symmetrical Gaussian quadrature rules for the triangle," *Int. J. Numer. Methods Eng.*, vol. 21, no. 6, pp. 1129-1148, Jun. 1985.